duced by β-CCE (Figs. 1 and 2). The antagonist had no significant behavioral or physiological actions when administered alone (Fig. 1). Diazepam (1 to 2 mg/kg) also markedly attenuated the behavioral and physiological effects of β-CCE.

β-Carboline-3-carboxylic acid ethyl ester possesses a high affinity for brain benzodiazepine receptors (*4*), antagonizes many of the pharmacological actions of benzodiazepines (*5*), and does not elicit overt changes in behavior in rodents when administered alone. However, in a more sensitive test of social interaction (*11*), this compound exerted an action opposite that of the benzodiazepines, which has been interpreted as "anxiogenic." These results suggest that at least three distinct classes of drugs are capable of binding to the benzodiazepine receptor. Drugs of the first class, historically called agonists, produce anxiolytic and anticonvulsant effects. An example is diazepam. The second class comprises antagonists with no intrinsic activity at moderate doses, such as Ro 15-1788 and CGS-8216 (*12*). The third class includes "active" antagonists, such as β-CCE and related β-carboline esters. Our data suggest that drugs of the first two classes effectively antagonize the pharmacological actions of the third (*12*).

In the rhesus monkey β-CCE elicits a profound elevation in the concentrations of circulating stress-related hormones, such as cortisol and the catecholamines epinephrine and norepinephrine. Increases in plasma cortisol and catecholamines are associated with anxiety in humans (*13*) and with experimental anxiety (such as conflict behavior) in animals (*14*). Benzodiazepines decrease stress-induced elevations in cortisol and catecholamines in both animals and humans (*15*). Concomitant with the endocrine changes elicited by β-CCE are the somatic manifestations, such as increases in heart rate and blood pressure. Furthermore, a wide range of behaviors were elicited by β-CCE, many of which have been proposed to represent "anxious" behavior in other primate models of anxiety, such as mother-infant separation (*16*) and direct stimulation of the locus ceruleus (*17*).

Since anxiety is an emotional state characterized by feelings of impending danger or fear, it is impossible to unequivocally demonstrate the presence or absence of anxiety in any animal. Nevertheless, the endocrine, somatic, and behavioral effects of β-CCE are reminiscent of changes observed in anxious patients and in animals and humans exposed to anxiety-provoking or stressful situations (*13–17*). The blockade of the behavioral and physiological actions of β-CCE by the benzodiazepine receptor antagonist Ro 15-1788 strongly suggests that the actions of β-CCE are mediated through the benzodiazepine receptors. Thus, administration of β-CCE to animals may represent a reliable and reproducible model of human anxiety and, as such, could be valuable in studying the postulated role of anxiety and stress in a variety of human diseases, including cardiovascular, ulcerative, and neoplastic disorders (*18*). Taken together, our results suggest that the benzodiazepine–γ-aminobutyric acid receptor complex not only mediates the pharmacological actions of the benzodiazepines, but also subserves the affective and physiological expression of anxiety.

PHILIP T. NINAN
Clinical Neuroscience Branch, National Institute of Mental Health, Bethesda, Maryland 20205
THOMAS M. INSEL
ROBERT M. COHEN
Clinical Neuropharmacology Branch, National Institute of Mental Health
JAMES M. COOK
Department of Chemistry, University of Wisconsin, Milwaukee 53201
PHIL SKOLNICK
Laboratory of Bioorganic Chemistry, National Institute of Arthritis, Diabetes, and Digestive and Kidney Diseases, Bethesda, Maryland 20205
STEVEN M. PAUL
Clinical Neuroscience Branch, National Institute of Mental Health

References and Notes

1. J. F. Tallman, S. M. Paul, P. Skolnick, D. W. Gallager, *Science* **207**, 274 (1980); S. M. Paul, P. Marangos, P. Skolnick, *Biol. Psychiatry* **16**, 213 (1981).
2. P. Skolnick and S. M. Paul, *Int. Rev. Neurobiol.* **23**, 103 (1982).
3. S. M. Paul and P. Skolnick, in *Anxiety: New Research and Changing Concepts*, D. Klein and J. Rabkin, Eds. (Raven, New York, 1981), p. 215.
4. C. Braestrup, M. Nielsen, C. Olsen, *Proc. Natl. Acad. Sci. U.S.A.* **77**, 2288 (1980).
5. S. Tenen and J. Hirsch, *Nature (London)* **288**, 609 (1980); P. Cowen, A. Green, D. Nuh, I. Martin, *ibid.* **290**, 54 (1981).
6. W. Hunkeler, M. Mohler, L. Pieri, P. Polc, E. Bonetti, R. Cumin, R. Schaffner, W. Haefely, *ibid.* **290**, 514 (1981); P. Polc, J.-P. Laurent, R. Scherschlicht, W. Haefely, *Naunyn-Schmiedeberg's Arch. Pharmacol.* **316**, 317 (1981).
7. B. H. Natelson, N. Krasnejor, J. W. Holaday, *J. Comp. Physiol. Psychol.* **90**, 958 (1976); C. F. Farver, D. De Wied, P. T. K. Toivola, *J. Endocrinol.* **79**, 247 (1978).
8. All drugs were dissolved or suspended in 20 percent Emulphor (GAF Corp.) diluted 1:1 with 95 percent ethanol and in 80 percent sterile saline in a volume of 10 ml for β-CCE and 5 ml for Ro 15-1788. The dose of β-CCE used (2.5 mg/kg) was empirically chosen on the basis of (i) its reported affinity for the benzodiazepine receptor (≃ 1 n*M*) and (ii) recent studies from our laboratory demonstrating that β-CCE degrades very rapidly when incubated with rat plasma in vitro at 37°C [W. Mendelson, M. Cain, J. Cook, S. M. Paul, P. Skolnick, in *Beta-Carbolines and Tetraisoquinolines*, E. Usdin, J. Barchas, F. Bloom, Eds. (Liss, New York, 1982), p. 253].
9. D. S. Goldstein, G. Fuerstein, J. L. Izzo, I. J. Kopin, H. R. Keiser, *Life Sci.* **28**, 467 (1981).
10. Plasma epinephrine concentrations rose from 171 ± 23 to 1542 ± 505 pg/ml (means ± standard errors) and norepinephrine levels rose from 545 ± 109 to 1476 ± 467 pg/ml after β-CCE administration (Fig. 2).
11. S. File, in *Pharmacology of Benzodiazepines*, E. Usdin, P. Skolnick, J. F. Tallman, D. Greenblatt, S. M. Paul, Eds. (Macmillan, London, in press).
12. M. Schweri, M. Cain, J. Cook, S. M. Paul, P. Skolnick, *Pharmacol. Biochem. Behav.* **17**, 457 (1982); C. Braestrup, R. Schmiechen, G. Neef, M. Nielsen, E. N. Petersen, *Science* **216**, 1241 (1982).
13. E. J. Sachar, *Prog. Brain Res.* **32**, 36 (1970).
14. A. S. Lippa, E. N. Greenblatt, R. W. Pelham, in *Animal Models in Psychiatry and Neurology*, I. Hanin and E. Usdin, Eds. (Pergamon, New York, 1979), p. 279.
15. G. Lefur, F. Guilloux, N. Mitrani, J. Mizoule, A. Uzan, *J. Pharmacol. Exp. Ther.* **211**, 305 (1979); R. Lahiti and C. Barsuhn, *Psychopharmacology* **35**, 215 (1979).
16. S. J. Suomi, G. W. Kraemer, C. M. Baysinger, R. D. DeLizio, in *Anxiety: New Research and Changing Concepts*, D. F. Klein and J. Rabkin, Eds. (Raven, New York, 1981), p. 174.
17. D. E. Redmond and Y. H. Huang, *Life Sci.* **25**, 2149 (1979).
18. V. Riley, *Science* **212**, 1100 (1981); J. P. Henry and G. A. Santisteban, *Atherosclerosis* **14**, 203 (1971); J. W. Mason, in *Frontiers in Neurology and Neuroscience Research*, P. Seeman and G. M. Brown, Eds. (Univ. of Toronto Press, Toronto, 1974), p. 168.
19. We thank S. Rapaport, J. Aloi, and C. McLellan for technical assistance, J. Colison for statistical analysis, and E. Churgin and T. Welsh for typing the manuscript.

18 August 1982; revised 29 October 1982

Monoclonal Antibodies in the Lymphatics: Toward the Diagnosis and Therapy of Tumor Metastases

Abstract. *Monoclonal antibodies subcutaneously injected into mice track to regional lymph nodes and specifically label target cells there. The lymphatic route of administration can be expected to provide much higher sensitivity, higher target-to-background ratio, faster localization, and lower toxicity than the intravenous route when the aim is to diagnose or treat tumor metastases or lymphoma in the lymph nodes.*

Monoclonal antibodies (*1*) have been touted as a modern incarnation of Paul Ehrlich's "magic bullet." With radionuclides attached, they appear clinically useful for gamma camera imaging of tumors (*2*). In the realm of therapy, they may be able to mobilize endogenous defenses or to direct an attached drug, toxin, or radionuclide to tumor cells (*3*). Thus far, monoclonal antibodies have

0036-8075/82/1224-1334$01.00/0 Copyright © 1982 AAAS

been administered in vivo almost exclusively by intravenous injection (*4*), on the reasonable grounds that they can leak out of the blood vessels to expose nearly every tissue. However, for reasons to be discussed here, it would be highly advantageous if anatomic localization could be added to the inherent antigenic specificity of the antibodies.

One anatomic compartment of great importance in oncology is the lymphatic system—the problem being to diagnose and treat early lymph node metastases. Figure 1 shows the fate of a molecule or particle after interstitial (subcutaneous) injection. If not phagocytosed or bound to tissues locally, small molecules can pass directly into the blood capillaries. Large molecules and particles do not readily enter the blood vessels and instead pass into lymphatic channels through clefts in the lymphatic endothelium (*5*). A protein the size of monomeric immunoglobulin G (IgG) passes principally into the lymph. It then traverses one or more lymph nodes before entering the blood stream through the thoracic duct or other lymphatic trunks. In transit through the nodes, it can associate with macrophages, endothelial cells, normal lymphocytes, or tumor cells. Radioactively labeled colloids have been used nonspecifically to visualize disruptions of lymphatic drainage by tumor cells in pelvic, inguinal, axillary, and internal mammary nodes (*6–8*); they have also been used in several attempts at nonspecific therapy in the lymphatics (*9*).

Partially purified antiserums to ferritin (*10*) and carcinoembryonic antigen (*11*) have been injected into patients for imaging of tumors in lymph nodes. However, the use of human subjects made it difficult to do specificity control experiments, and the lack of monoclonal homogeneity coupled with the variability of tumors precluded quantitative pharmacokinetic analysis. The results could not be used to optimize delivery. Hence, we have started from the other end of the methodological spectrum, using monoclonal antibodies well characterized in their equilibrium and kinetic binding properties. We are working initially with antibodies to normal cell determinants because they provide reproducible systems with which to develop the pharmacokinetic principles for attacking tumors in the nodes.

Most of our studies were done with 36-7-5, a murine monoclonal Ig_{2a},κ antibody specific for the mouse class I major histocompatibility antigen H-2K^k (*12*). The antigen K^k is expressed on over 90 percent of the lymphocytes of mouse strains that bear it and (generally at lower levels) on other cell types in those animals. The antibody binds specifically to a single class of sites on K^k-positive spleen cells (from B10.A and B10.BR mice) to a maximum extent of about 2.4×10^4 antibody molecules per cell at 0°C. The affinity, association rate constant, and dissociation rate constant are $3 \times 10^8 M^{-1}$, $3 \times 10^6 M^{-1}$ min^{-1}, and $\sim 10^{-3}$ min^{-1}, respectively (*13*). Pharmacokinetic analysis indicates that the affinity and dissociation constant will figure prominently in optimizing lymphatic delivery of antibodies (*14*).

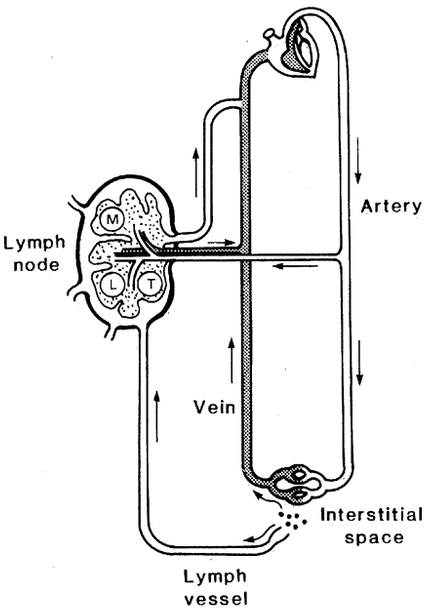

Fig. 1. Schematic view of the passage of a molecule or particle from an interstitial injection site into blood or lymph. In lymph nodes the particle may become associated with macrophages (*M*), lymphocytes and other normal cells of the node (*L*), or tumor cells (*T*).

To assess delivery to the nodes, we injected ^{125}I-labeled 36-7-5 into the hind foot pads of K^k-positive mice (B10.A females) and K^k-negative mice (C57BL/6 females). Results were essentially identical when we used B10.BR as the positive strain or C57BL/10, B10.D2, or B10.P as the negative strain. Figure 2 shows the distribution of labeled antibody observed when the animals were killed 2 hours after injection. The popliteal nodes of the B10.A mice contained 14 percent of the injected dose (or 32 percent of the dose absorbed from the feet), whereas in the C57BL/6 mice these nodes contained only 0.28 percent (ratio, 50:1). The lumbar and renal nodes of B10.A mice were also labeled, whereas distant nodes were not. The ratio of popliteal to cervical node radioactivity was 840:1, indicating that the nodes had been labeled through regional lymph flow, not the bloodstream. The entire liver bound less antibody than did the K^k-positive popliteal nodes. Since each node weighs 0.8 to 1.0 mg, the ratio of popliteal node to liver radioactivity was more than 1000:1 on the basis of counts per minute per milligram of tissue. The average concentration of 36-7-5 in the feet was 41 times less than that in the popliteal nodes. More counts were measured in the feet of B10.A animals than in the feet of C57BL/6 animals, indicating specific association of the antibody with K^k-bearing cells there. The blood of K^k-positive mice contained only 2 percent of the injected dose, whereas 42 percent was still circulating in the blood of the K^k-negative controls. Disruption of the popliteal nodes after subcutaneous injection of the antibody showed approximately half of the counts to be associated with lympho-

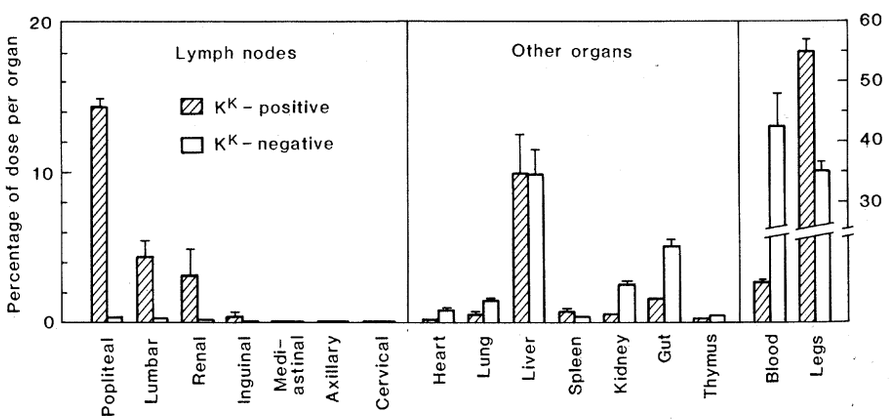

Fig. 2. Distribution of ^{125}I-labeled antibody to H-2K^k 2 hours after injection in both foot pads. Mice matched for age and weight were anesthetized briefly with ether and injected with 50 μl of a solution containing 2.7 pmole of protein A–purified antibody labeled with ^{125}I by the chloramine T procedure to a specific activity of 8.3×10^{14} dpm/mmole. Bars represent mean data for groups of three mice, with standard errors indicated where large enough to show. Sodium dodecyl sulfate–gel electrophoresis, performed after solubilization of popliteal node cells with NP40 detergent, showed that the ^{125}I counts represented primarily intact IgG.

cytes, half with macrophages and stroma. This binding was clearly specific, since it was minimal in K^k-negative mice.

Very different results were obtained after intravenous injection of the antibody. Only 0.023 and 0.012 percent of the injected radioactivity was present in the popliteal nodes of K^k-positive and K^k-negative mice, respectively, after 2 hours—0.005 and 0.003 percent after 72 hours.

As a second type of specificity control, we used ^{125}I-labeled 27-11-13, a monoclonal antibody of the same subclass as 36-7-5 but specific for the histocompatibility antigens D^b and D^d rather than K^k (*15*). B10.BR mice (D^k-positive) showed only background levels of uptake, whereas C57BL/10 (D^b-positive) and B10.A (D^d) showed specific uptake in the regional nodes.

The first clinical application of monoclonal antibodies in the lymphatics will probably be immunoscintigraphic imaging of solid tumor metastases and lymphomas. The time course of 36-7-5 distribution, as observed by lymphatic immunoscintigraphy, is shown in Fig. 3, A and B. In K^k-positive mice the popliteal and lumbar nodes were clearly visualized 20 minutes after injection. The images began to fade within 24 hours. The thyroid accumulated iodine within several hours of injection (such uptake could be suppressed by prior treatment with KI if desired). After 17 hours a large number of counts appeared in the bladder. When we injected labeled 36-7-5 into only one foot pad, the contralateral popliteal and lumbar nodes acquired less than 1 percent as much radioactivity as the ipsilateral nodes. With the K^k-negative strain, injection into the foot pads failed to show the regional nodes clearly. Intravenous injection of antibodies did not visualize the nodes in either strain (Fig. 3, C and D). In parallel experiments, injection of $(Fab')_2$ fragments of 36-7-5 gave essentially the same pattern of specific node localization as whole IgG (*16*).

Our studies with 36-7-5 and 27-11-13 strongly suggest that minor subpopulations of cells in a node can be labeled selectively. We confirmed this with a fluorescein-labeled rat IgG_1 antibody to Lyt-2 (clone 53-6.7) (*17*). After being injected into the foot pads, it labeled 19 percent of the popliteal node cells (as assessed by fluorescence microscopy and flow microfluorimetry), the same value we obtained when labeling popliteal node cells in vitro. Thus, it should be possible to label lymph node lymphoma cells, which tend to be distributed in the same way as their normal counterparts in the architecture of the node.

The major limitations of lymphatic immunodiagnosis and immunotherapy are (i) the regional nature of the approach and (ii) its restriction to lymph node metastases still small enough to permit lymph flow. With respect to the first limitation, however, a reasonable number of injection sites would suffice to reach most nodes. We find, for example, that injections of antibody to K^k into mouse forepaws and ears label axillary and cervical nodes, respectively. Similarly, colloids have been injected into the hand to visualize human axillary nodes, and subcostally to reach the internal mammary chain (*7*). With respect to the second limitation, it may be especially important to reach micrometastases representing early stages of tumor spread, both to assess the stage of the disease and for therapy. One can envision combined diagnostic modalities in which an antibody reactive to the tumor is used to scan for small metastases, and a nonspecific marker, perhaps an antibody to normal node cells, is used to identify gross disruptions of the lymphatic chain.

The potential advantages of the lymphatic route are equally clear. Using immunoscintigraphy, we are able to visualize far less than 1 mg of murine cells, as opposed to the hundreds of milligrams typically imaged by the intravenous route. The dose required for visualization is much lower than with intravenous administration, and the nodes are visualized in 20 minutes, compared with the 6 to 96 hours typical for imaging by the intravenous route. (Rapid visualization would greatly ease the logistics of diagnostic imaging. Second or third agents could be injected sequentially.) Selective delivery to the lymphatic compartment would dramatically reduce background interference and decrease interaction with circulating antigens and nontumor cells that express the antigen. The H-2 determinant used in this study provides a model for such tumor-associated (as opposed to tumor-specific) antigens. Furthermore, localization in a compartment can be expected to decrease such un-

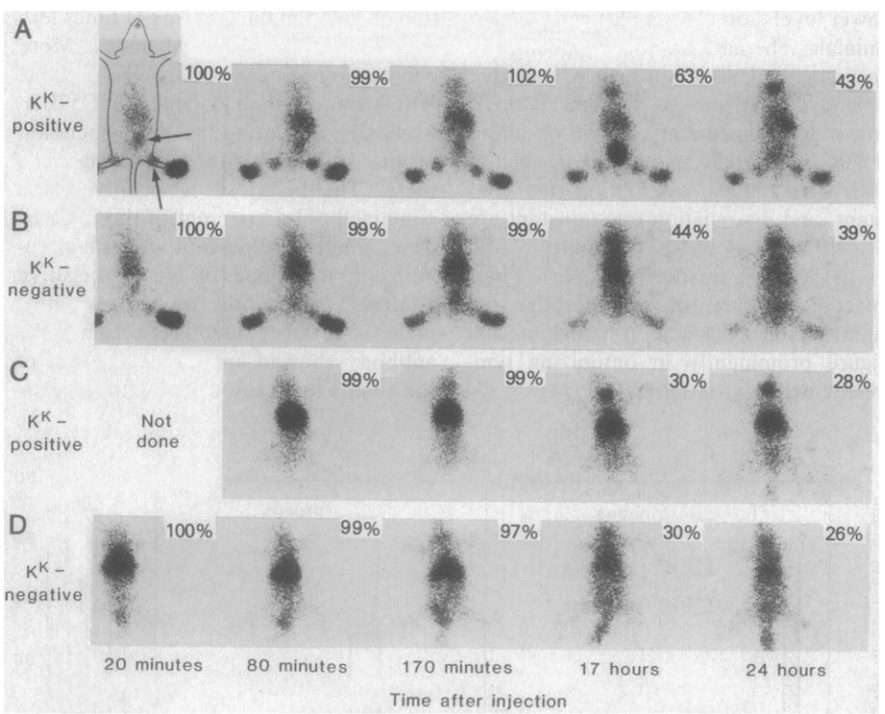

Fig. 3. Scintigraphic images of H-$2K^k$–positive (B10.BR) and H-$2K^k$–negative (B10.P) mice injected subcutaneously (A and B) and intravenously (C and D) with ^{125}I-labeled 36-7-5. Values are percentages of the dose remaining in the body. In the K^k-positive mouse injected subcutaneously (A), the most prominent spots represent the foot pads. Popliteal and lumbar nodes (arrows) are also prominent. We determined the organ corresponding to each labeled spot by killing the animals and then imaging repeatedly as various organs were removed. Injections were done as described in the legend to Fig. 2, except that the solution contained 2.9 pmole of protein A–purified IgG labeled to a specific activity of 5.8×10^{15} dpm/mmole. The activity seen in the tails of intravenously injected mice at later times probably reflects nonspecific accumulation at the site of puncture. Each image consisted of 15,000 counts, recorded (at an approximate efficiency of 7×10^{-4}) with a Raytheon Anger gamma camera having a 0.25-inch pinhole collimator. Computer integrations of each image (corrected for spherical aberration and background) were used to estimate the percentage of dose remaining as a function of time and also the amount of ^{125}I per organ.

wanted side effects as the deposition of immune complexes in the kidney. Whether or not toxic side effects prove to be a problem clinically with naked antibodies, they will almost certainly be significant with antibody-coupled drugs, toxins, or alpha-emitters. If necessary, local toxicity at the point of injection could be reduced by distributing the dose over a number of local sites.

Likely candidates for lymphatic immunodiagnosis and immunotherapy are mammary, lung, and colon carcinomas, lymphomas, and melanomas. With melanomas, for example, one would eliminate interference from antigenic determinants on normal melanocytes in the skin by using the lymphatic route to metastases in the regional nodes.

In the studies reported here, normal cells were used as targets in order to establish the principles for delivering antibodies to lymph nodes. More recently, we obtained specific localization of an antitumor antibody in guinea pig nodes containing metastases from a hepatocarcinoma (*18*).

JOHN N. WEINSTEIN
Laboratory of Mathematical Biology, National Cancer Institute, Bethesda, Maryland 20205
ROBERT J. PARKER
Laboratory of Chemical Pharmacology, National Cancer Institute
ANDREW M. KEENAN
Department of Nuclear Medicine, National Institutes of Health, Bethesda, Maryland 20205
STEVEN K. DOWER
Immunology Branch, National Cancer Institute
HERBERT C. MORSE III
Laboratory of Viral Diseases, National Institute of Allergy and Infectious Diseases, Bethesda, Maryland 20205
SUSAN M. SIEBER
Laboratory of Chemical Pharmacology, National Cancer Institute

References and Notes

1. G. Kohler and C. Milstein, *Nature (London)* **256**, 495 (1975).
2. G. Levine, B. Ballou, J. Reiland, D. Solter, L. Gmerman, T. Hakala, *J. Nucl. Med.* **21**, 570 (1980); D. A. Scheinberg, M. Strand, O. A. Gansow, *Science* **215**, 1511 (1982). For a review of the literature on imaging with antiserums (not monoclonals), see D. Pressman, *Cancer Res.* **40**, 2960 (1980).
3. R. A. Miller, D. G. Maloney, R. Warnke, R. Levy, *N. Engl. J. Med.* **306**, 517 (1982).
4. L. L. Houston, R. C. Nowinski, I. D. Bernstein, *J. Immunol.* **125**, 837 (1980); M. R. Tam, I. D. Bernstein, R. C. Nowinski, *Transplantation* **33**, 269 (1982).
5. L. V. Leak, *J. Cell Biol.* **50**, 300 (1971).
6. A. I. Sherman, M. Ter-Pogossian, E. C. Tocus, *Cancer* **6**, 1238 (1953); A. Alavi, M. M. Staum, B. F. Shesol, P. H. Bloch, *J. Nucl. Med.* **19**, 422 (1978); D. A. Goodwin, R. A. Finston, L. G. Colombetti, J. E. Beaver, H. Hupf, *Radiology* **94**, 175 (1970).
7. G. N. Ege, *Radiology* **118**, 101 (1976).
8. W. Hauser, H. L. Atkins, P. Richards, *ibid.* **92**, 1369 (1969).
9. A. I. Sherman, M. Bonebrake, W. M. Allen, *Am. J. Roentgenol. Radium Ther. Nucl. Med.* **66**, 624 (1951); P. F. Hahn and E. L. Carothers, *Br. J. Cancer* **5**, 400 (1951).
10. S. E. Order, W. D. Bloomer, A. G. Jones, W. D. Kaplan, M. A. Davis, S. J. Adelstein, S. Hellman, *Cancer* **35**, 1487 (1975).
11. F. H. DeLand, E. E. Kim, R. L. Corgan, S. Casper, F. J. Primus, E. Spremulli, N. Estes, D. M. Goldenberg, *J. Nucl. Med.* **20**, 1243 (1979); F. H. DeLand, E. E. Kim, D. M. Goldenberg, *ibid.* **21**, 805 (1980); G. N. Ege and M. J. Bronskill, *ibid.*, p. 804.
12. D. H. Sachs, N. Mayer, K. Ozato, in *Monoclonal Antibodies and T-Cell Hybridomas*, U. Hammerling and J. F. Kearney, Eds. (Elsevier, Amsterdam, 1981), p. 95.
13. Binding was analyzed by S. K. Dower *et al.* (in preparation) with the methods of D. M. Segal and E. Hurwitz, *J. Immunol.* **118**, 1338 (1977).
14. D. Covell, J. N. Weinstein, M. Steller, A. M. Keenan, S. M. Sieber, R. J. Parker, in preparation.
15. K. Ozato and D. H. Sachs, *J. Immunol.* **126**, 317 (1981).
16. R. J. Parker, J. N. Weinstein, M. Steller, A. M. Keenan, D. Covell, S. K. Dower, S. M. Sieber, in preparation.
17. J. A. Ledbetter and L. A. Herzenberg, *Immunol. Rev.* **47**, 63 (1979).
18. J. N. Weinstein, R. J. Parker, M. Steller, K. Hwang, M. Key, D. Covell, S. M. Sieber, in preparation.
19. We thank M. Steller for valuable technical assistance; D. Sachs, K. Ozato, and J. Bluestone for providing antibodies; E. Jones for gamma camera facilities; and D. Segal, J. Titus, P Henkart, S. Sharrow, S. Epstein, M. Knode, D. Covell, and R. Dedrick for advice and assistance.

27 July 1982; revised 19 October 1982

The Neuroanatomy of Amnesia: Amygdala-Hippocampus versus Temporal Stem

Abstract. *Using a task known to be sensitive to human amnesia, we have evaluated two current hypotheses about which brain regions must be damaged to produce the disorder. Monkeys with bilateral transections of the white matter of the temporal stem were unimpaired, but monkeys with conjoint amygdala-hippocampal lesions exhibited a severe memory deficit. The results indicate that the hippocampus, amygdala, or both, but not the temporal stem, are involved in memory in the monkey and suggest that a rapprochement between the findings for the human and the nonhuman primate may be close at hand.*

Damage to the medial temporal region of the human brain has been known for many years to cause a profound amnesic syndrome, and the critical structure in bitemporal amnesia has been presumed to be the hippocampal formation (*1*). Yet studies of nonhuman primates with surgical lesions of the hippocampus, which

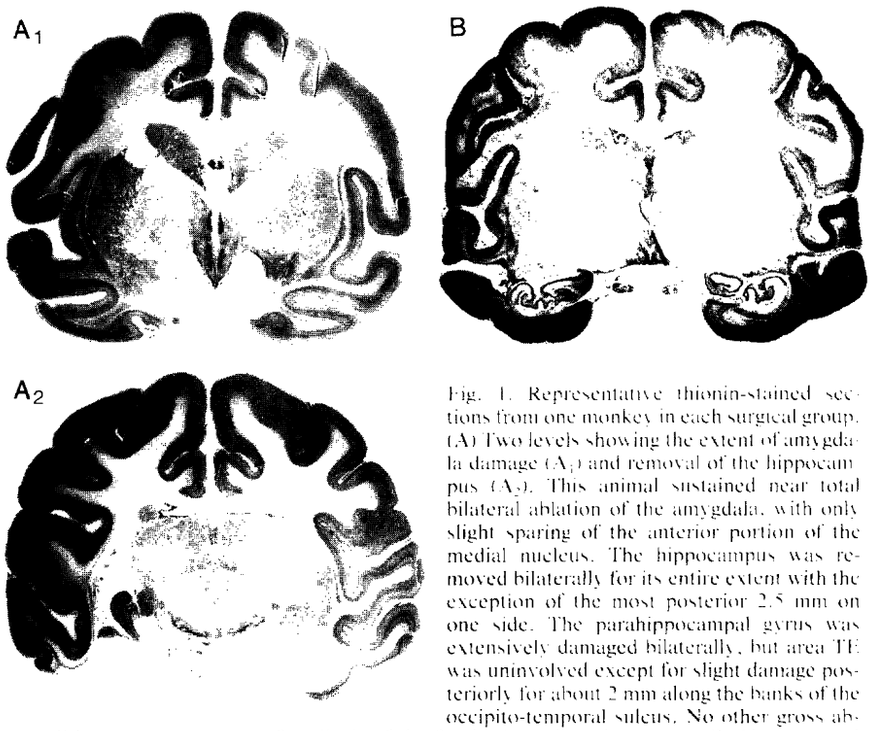

Fig. 1. Representative thionin-stained sections from one monkey in each surgical group. (A) Two levels showing the extent of amygdala damage (A_1) and removal of the hippocampus (A_2). This animal sustained near total bilateral ablation of the amygdala, with only slight sparing of the anterior portion of the medial nucleus. The hippocampus was removed bilaterally for its entire extent with the exception of the most posterior 2.5 mm on one side. The parahippocampal gyrus was extensively damaged bilaterally, but area TE was uninvolved except for slight damage posteriorly for about 2 mm along the banks of the occipito-temporal sulcus. No other gross abnormalities were seen except for gliosis of the fornix throughout its extent. (B) The temporal stem was transected for an anterior-posterior extent of approximately 15 mm from just behind the temporal pole to approximately the middle level of the lateral geniculate nucleus. The upper bank as well as the cortex at the fundus of the superior temporal sulcus was removed for most of the extent of the lesion. The hippocampus was undamaged throughout its extent.

0036-8075/82/1224-1337$01.00/0 Copyright © 1982 AAAS